Data in Brief 64 (2026) 112304

Contents lists available at ScienceDirect

Data in Brief

journal homepage: www.elsevier.com/locate/dib

Data Article

A dataset to support wildland fire and fuel management in Greece created with stochastic wildfire simulations

Palaiologos Palaiologou[a,*], Christos Giannakopoulos[b], Christos Vasilakos[c], Stavros Sakellariou[d], Marcos Rodrigues[e], Anna Karali[b], George Katavoutas[b], Konstantinos V. Varotsos[b], Olga Roussou[c], Pere Joan Gelabert[f], Adrián Jiménez-Ruano[g], Giannis Lemesios[b], Antoni Trasobares[h], Mark Finney[i], Kostas Kalabokidis[c]

[a] *Agricultural University of Athens, Department of Forestry and Natural Environment Management, Karpenisi, Greece*
[b] *National Observatory of Athens, Institute for Environmental Research and Sustainable Development, Athens, Greece*
[c] *University of the Aegean, Department of Geography, Mytilene, Greece*
[d] *Department of Civil and Environmental Engineering, Brunel University of London, Uxbridge, United Kingdom*
[e] *Department of Geography and Land Management, University of Zaragoza, Zaragoza, Spain*
[f] *Department of Agriculture and Forest Engineering, University of Lleida, Lleida, Spain*
[g] *Technosylva Inc, CA, USA*
[h] *Forest Science and Technology Centre of Catalonia, Solsona, Lleida, Spain*
[i] *Missoula Fire Sciences Laboratory, MT, USA*

ARTICLE INFO

Article history:
Received 7 October 2025
Revised 11 November 2025
Accepted 17 November 2025
Available online 26 November 2025

Dataset link: A dataset to support wildland fire and fuel management in Greece created with stochastic wildfire simulations (Original data)

ABSTRACT

The potential spread and intensity of wildfires can be estimated with fire modelling simulators that produce valuable datasets which can be used during the prevention and suppression stages by fire management agencies. In the absence of observational data for all potential ignition sources, since a fire has not yet occurred or has burned many decades ago, fire behavior algorithms such as the Minimum Travel Time incorporated in the FSim simulator can be used to reveal these hidden fire patterns and trajectories. FSim is widely used in the USA for that purpose and its outputs, i.e.,

DOI of original article: 10.1016/j.geomat.2024.100036
* Corresponding author.
E-mail address: palaiologou@aua.gr (P. Palaiologou).
Social media: @Paleologos2 (P. Palaiologou)

https://doi.org/10.1016/j.dib.2025.112304

Keywords:
FSim
Fire intensity
Burn probability
Ignition probability
Fire perimeters
Conditional flame length
Fuel models
Minimum travel time algorithm

fire perimeters, ignition locations, fire intensity and burn probability are used in numerous assessments and applications, from fireshed delineation and community protection planning to exposure calculations of wildfire risk by the reinsurance industry. However, no country-scale application exists for Europe, due to the previous lack of essential model input data at an adequate spatial resolution (~100 m), specifically fuel models, canopy base height and canopy bulk density. The EU H2020 funded project "FIRE-RES" filled that gap and produced the necessary input dataset at a pan-European level, enabling the first large scale nationwide stochastic fire behavior modelling application for Greece. The methods can be replicated and the datasets produced and presented in this work can be produced for every continental EU country. After retrieving the necessary spatial datasets from on-line open access repositories, we assembled them to create a landscape file. Greece was divided into 23 Pyromes that are regions with similar vegetation, climate and fire behavior. Then, weather patterns were summarized in a format compatible with FSim using hourly data of air temperature, dewpoint temperature, incident solar radiation, precipitation, and northward and eastward wind components for the years 2000–2021 from the state-of-the-art global reanalysis dataset ERA5-Land. Ignition locations were distributed across each Pyrome using an ignition probability grid, ensuring that we simulated enough fires so that each burnable pixel of the landscape experiences at least one event. Simulations were validated by comparing the historic fire size distribution of each Pyrome with the simulated one. The dataset includes the burn probability and conditional flame length rasters at 100 m spatial resolution, and the 3.65 million fire perimeters and ignition locations in vector format. In addition, we provide those input datasets that are not available in other repositories, specifically the modified fuel models and the ignition probability rasters. The data provided in this article offers a valuable resource for fire management and civil protection agencies, enabling them to understand the fire size potential of each area and the expected burning intensity. In addition, metanalyses of fire perimeters intersecting them with settlement boundary polygons can provide their exposure profiles to inform fuel treatment and community protection plans. Risk profiles may also be produced by linking exposure with expected fire intensity, even at building level, providing useful datasets for insurance purposes and spatial planning.

Specifications Table

Subject	Earth & Environmental Sciences
Specific subject area	Stochastic wildfire simulation modelling and estimation of key wildland fire behavior metrics for Greece
Type of data	Analyzed & Processed, Spatial Datasets (raster and vector format)

(*continued on next page*)

Data collection	Simulation input data were collected from the Pan-European Fuel Map Server (https://www.cirgeo.unipd.it/fire-res/app/) [1]. Fuel models were assigned at the different fuel types using datasets from the Copernicus Land Monitoring Service such as elevation, imperviousness, grasslands and herbaceous 2021, the CLCplus Backbone 2021, and information retrieved from local forest management plans from different Greek regions. The research group knowledge from past inventories ensured that the assigned fuel models matched the on-ground conditions. Weather parameters retrieved from the state-of-the-art global reanalysis dataset ERA5-Land, available in the C3S Climate Data Store.
Data source location	The stochastic fire simulations cover the country of Greece. All input datasets used are listed in the reference list file in the repository. Data are stored at: University of the Aegean, Department of Geography, Mytilene 81,132, Lesvos Island, North Aegean Region, Greece
Data accessibility	Repository name: Zenodo Data identification number: https://doi.org/10.5281/zenodo.17579289 Direct URL to data: https://zenodo.org/records/17579289
Related research article	Kutchartt, E., González-Olabarria, J.R., Aquilué, N., Garcia-Gonzalo, J., Trasobares, A., Botequim, B., Hauglin, M., Palaiologou, P., Vassilev, V., Cardil, A., Navarrete, M.Á., Orazio, C., Pirotti, F. Pan-European fuel map server: an open-geodata portal for supporting fire risk assessment, Geomatica (2024) 100036. [1] https://doi.org/10.1016/j.geomat.2024.100036 Palaiologou, P., Kalabokidis, K., Day, M. A., Ager, A. A., Galatsidas, S., & Papalampros, L., 2022. Modelling fire behavior to assess community exposure in Europe: combining open data and geospatial analysis. ISPRS International Journal of Geo-Information, 11(3), 198. [2] https://doi.org/10.3390/ijgi11030198 Palaiologou, P., Kalabokidis, K. and Vasilakos, C., 2022. A geographical analysis of wildfire fuel characteristics by cover type in Greece. In Proceedings of "2nd AGROECOINFO", 30 June to 2 July 2022, Volos, Greece. [3]

1. Value of the Data

- The added value of this dataset lies in its potential to uncover hidden patterns of fire ignition, spread and exposure. In addition, the dataset enables quantitative estimates of the effectiveness of fuel treatments (e.g., how many potential fires can encounter the proposed fuel treatment projects) or the success of fire danger reduction campaigns (e.g., how many potential ignitions can occur inside the proposed fuel treatment projects). The wildfire simulation data produced encompasses the full range of meteorological conditions across the different Greek regions. It considers potential fire ignitions at locations that are not currently deemed as highly fire-prone or with expected small sized fires, which may in fact produce unprecedented large-scale events under extreme weather conditions. To do so, ignition locations were allocated even in areas that have not experienced a fire for more than 50 years with an average simulation density of 20 fires per km^2.
- The dataset includes 3.6 million simulated fire perimeters that cover the mainland of Greece and all the major populated islands. For each fire perimeter, simulated ignition points are provided along with information regarding fire size and number of buildings exposed. This information was used to construct spatial interpolated rasters that show which areas hold the higher potential to produce large fires (Fire Size Potential Index - FSPI) and the areas where fires can spread and reach populated places and structures (Structure Exposure Index – SEI), assuming a fire occurred at the location. Coupled with burn probability and conditional flame length rasters, these datasets can be combined among them or with other datasets to produce a better and comprehensive fire risk analysis. Furthermore, the provided data can be integrated with real-time and forecasted weather information to develop a new wildfire danger rating system tailored for Greece.
- The dataset can be used by the Electricity Network Moderators to identify sources over their network that may ignite large wildfires or expose nearby structures or communities. In addition, it can reveal which parts of the network have higher burn probability. This type of analysis is a simple geospatial analysis and can aid in the reduction of new ignitions and re-

ductions of maintenance and repair costs when targeted interventions for fuel risk reduction are applied.
- Researchers and public authorities can utilize the data to conduct further analysis to assess and rank settlements exposure, define their fireshed, identify the spatial origins of their exposure (e.g., at what land use types or ownerships), and where fuel treatment projects can be more effective in protecting these settlements. A probabilistic profile of the common directions from where fires can enter the boundary of each settlement can inform evacuation plans and escape routes.

2. Background

During the three major fire seasons in Greece (2007, 2021 and 2023), large fires erupted and shook the societal and political *status quo* regarding the way we confront, manage and live with fires, but also the way that wildfires reshaped biophysical and social realities. As we enter the era of mega-fires, we expect that similar wildfires will occur not only in regions prone to large fire propagation such as the Peloponnese, Attica and Evia, but also in high elevation ecosystems like those found in Central Greece and Epirus. By default, these ecosystems have reduced defenses from both the non-fire-resistant vegetation species that cover them and by the intense depopulation that led to land abandonment and in turn, fire deficiencies that enhance fuel accumulation. In the era of mega-fires, no region in Greece can be regarded as entirely "fire-proof". From this standpoint, it becomes essential to examine where potential future fires will ignite, how they will propagate and how they can affect populated places and other values-at-risk. One approach to examine this is through stochastic fire behavior modelling, i.e., producing millions of simulations of plausible wildfires. With fire simulations, settlement exposure or ecosystems risk can be estimated and used to plan and test for potential preventive measures that can reduce the estimated fire spread rate and intensity.

3. Data Description

The dataset in the Zenodo repository contains nine data layers, organized in a file geodatabase created with ESRI ArcMap version 10.4. All data are also provided as individual layers outside the geodatabase, the feature layers in the form of ESRI shapefiles, and the raster layers as .img (from ERDAS IMAGINE), using the ERDAS IMAGINE Hierarchal File Format (HFA) structure. Each .img raster layer has its own ancillary data, including the parameters height and width (rows and columns), layer type (continuous or thematic for Fuel Models), data type (32 Bit floating point, except for Fuel Models that are 8 Bit and unsigned integer), compression, and block size.

3.1. Pyromes

This is a polygon layer that shows the boundaries of the 23 macro-areas (Pyromes) of Greece (Fig. 1). The name of the layer inside the geodatabase is "Pyromes". A 20 km buffer zone outside the Greek boundaries was established, expanded to the countries of Albania, North Macedonia and Bulgaria, to account for the incoming and outgoing fires between these countries. The total area covered by the shapefile is 147,661 km^2. It is projected at the Projected Coordinate System: Greek_Grid (GCS_GGRS_1987); Projection: Transverse_Mercator; Datum: D_GGRS_1987. The Attribute Table of the dataset contains the following fields:

- Objectid: the unique ID of each Pyrome.
- Area_ha: The polygon area in hectares.
- Shape_Length: The length of each polygon in meters.

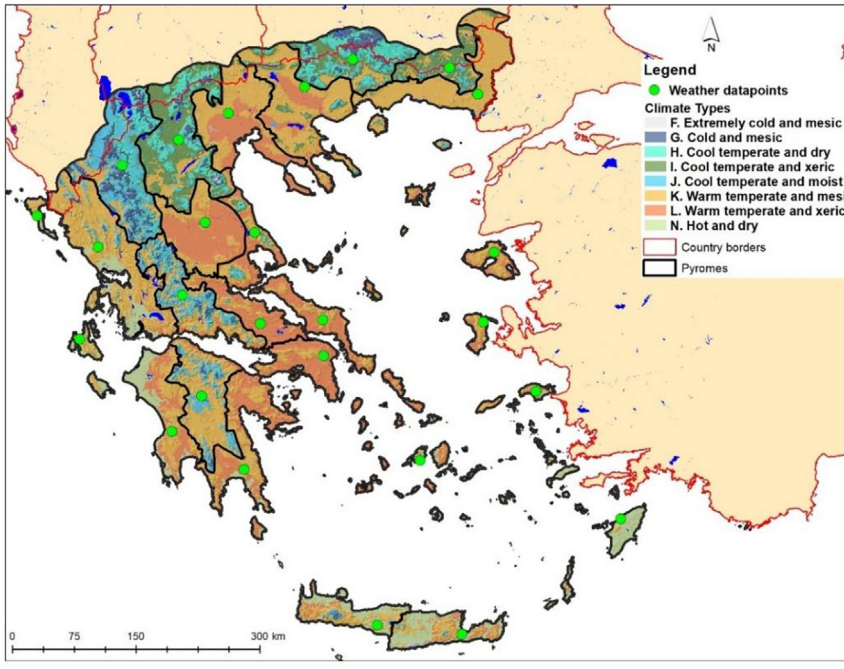

Fig. 1. Climate types of study area, including a buffer zone of 20-km at the northern borders of Greece.

- Shape_Area: The polygon area in square meters.
- Area_km2: The polygon area in square kilometers.
- Fires_true: The number of simulated fires at each Pyrome.
- Fires_area: The number of simulated fires each Pyrome should have if their number was defined by the area of the Pyrome following the rule of 17 ignitions per km^2.
- F_Seasons: The number of simulated fire seasons (Years) at each Pyrome.
- Pyrome: The name of each Pyrome, defined by the geographic name of the Greek Regions.

3.2. Fuel models

This is a raster layer of the entire Greek territory at 100 m spatial resolution (Fig. 2), with 9039 Columns and 7932 Rows, depicting the 24 assigned Scott and Burgan fuel models (FM) [4]. It contains data for the expanded 20 km boundary towards the northern neighboring countries of Greece. The name of the layer inside the geodatabase is “Fuel_Models”. It is projected at the Projected Coordinate System: Greek_Grid (GCS_GGRS_1987); Projection: Transverse_Mercator; Datum: D_GGRS_1987. The pixel type is 8 Bit unsigned integer. Null cell values were replaced with a non-burnable fuel model, i.e., 98, for computational efficiency during the simulations. The accompanying Layer file (.lyr) contains the proposed colors for the fuel set of fuel models.

3.3. Simulated fire perimeters

This is a polygon layer that shows the boundaries of the 3654,905 simulated fire perimeters with FSim Greece. Perimeter boundaries exceed the Greek boundary, and many entered the 20 km buffer zone. The name of the layer inside the geodatabase is “Fire_Perimeters”. It is

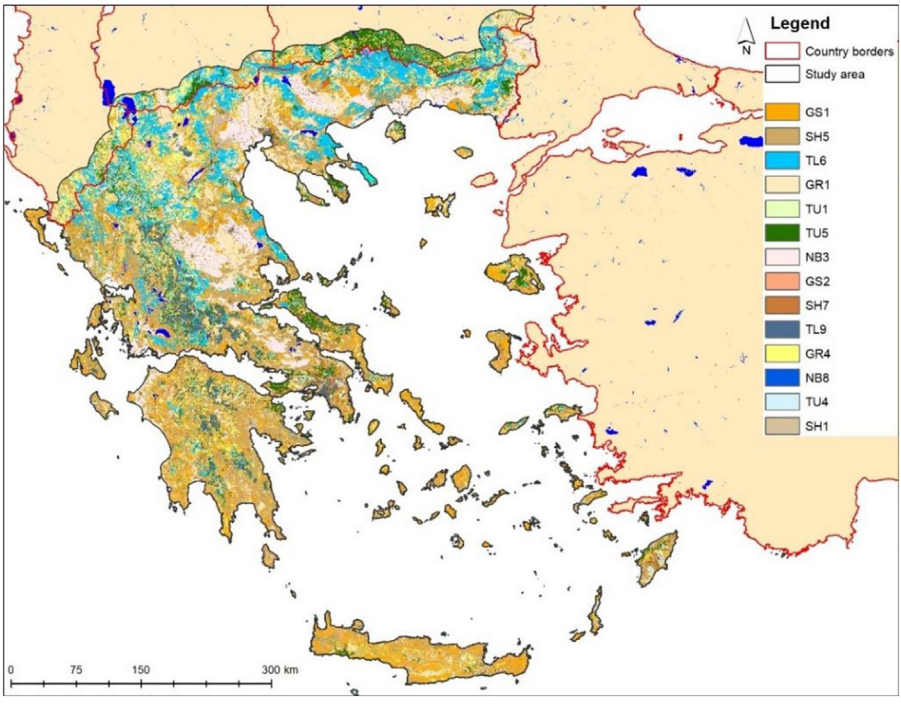

Fig. 2. Fuel models of study area, including a buffer zone of 20-km at the northern borders of Greece.

projected at the Projected Coordinate System: Greek_Grid (GCS_GGRS_1987); Projection: Transverse_Mercator; Datum: D_GGRS_1987. The attribute table provided indicates several important characteristics of each wildfire, including:

- ogc_fid: the unique identifier of each polygon for each Pyrome. Numbering is restarting from 1 among different Pyromes.
- Fire_id: is the unique fire number for a simulation. One fire can have more than one polygon. Numbering is restarting from 1 among different Pyromes.
- Season: the number of the fire season (Years) that the simulation was conducted. It can range from 0 to the number of total fire seasons that appear at the field “Years”.
- ignition_x/ ignition_y: are the coordinates of the fire’s ignition point.
- start_day: the Julian day of the fire start.
- num_days: is the number of days the fire burned during the simulation. This does not include any no-burn days (days below the 80th percentile ERC).
- Acres: the final fire size (acres) based on a count of pixels that burned (it does not include nonburnable pixels or pixels that did not burn but were entirely within the final fire perimeter). This field may vary from the fire’s area calculated from its associated perimeter.
- erc: is the ERC(G) on the start day of the fire.
- burn_minut: the minutes of active burning for each simulated fire.
- contain_re: the reason for the cessation of fire growth on the simulated fire.
- F_Seasons: the total number of iterations, defined as fire seasons of “years”, set for each Pyrome.
- Shape_Length: The length of each polygon in meters.
- Shape_Area: The polygon area in square meters.
- Area_ha: The polygon area in hectares.

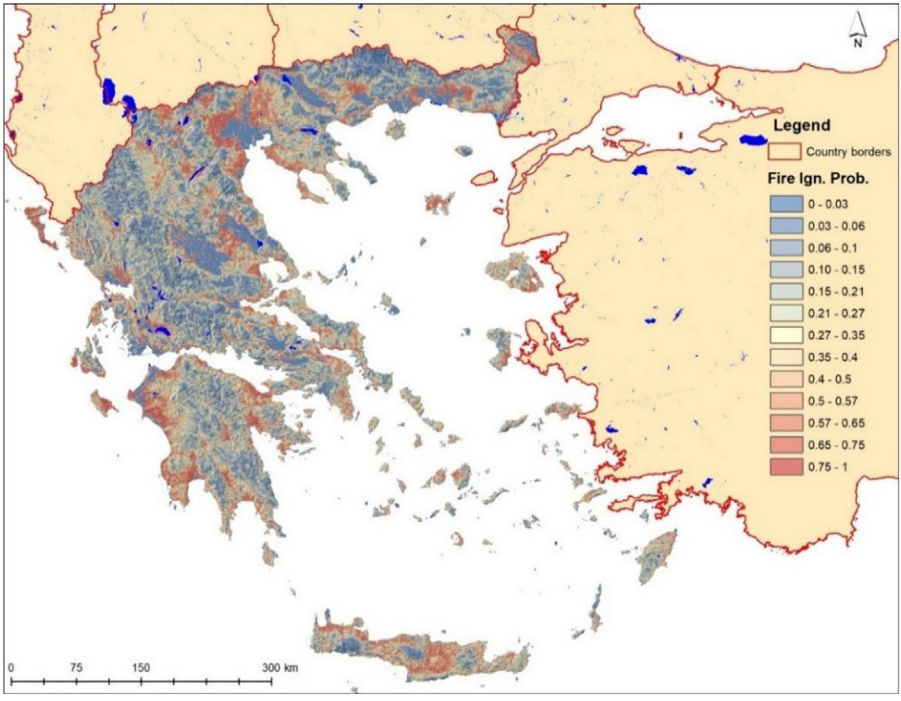

Fig. 3. Average fire ignition probability raster dataset.

- Fin_ID: the unique identifier across all polygons contained in this file. This field can be used to link fire perimeters with fire ignitions.
- Pyrome: the name of each Pyrome, defined by the geographic name of the Greek Regions.

3.4. Ignition probability

This is a raster layer of the entire Greek territory at 100 m spatial resolution (Fig. 3), with 9039 Columns and 7733 Rows, depicting the average human fire ignition probability (refer to subchapter 4.6 for a detailed description of the methods applied to generate it). The name of the layer inside the geodatabase is "Ignition_Prob". It is projected at the Projected Coordinate System: Greek_Grid (GCS_GGRS_1987); Projection: Transverse_Mercator; Datum: D_GGRS_1987. The pixel type is 32 Bit floating point. Null cell values were replaced with the value of zero. Pixels with non-burnable fuels from the Fuel Models rasters were used to assign a fire ignition probability value of zero to this raster. The accompanying Layer file (.lyr) contains the proposed colors for 13 classes (1: 0 – 0.03; 2: >0.03 – 0.06; 3: >0.06 – 0.1; 4: >0.1 – 0.15; 5: >0.15 – 0.21; 6: >0.21 – 0.27; 7: >0.27 – 0.35; 8: >0.35 – 0.4; 9: >0.4 – 0.5; 10: >0.5 – 0.57; 11: >0.57 – 0.65; 12: >0.65 – 0.75; 13: >0.75 – 1).

3.5. Simulated fire ignitions

This is a point layer that shows the ignition locations that FSim used to generate the fire perimeters for Greece. Ignition allocation exceeded in several instances the Greek boundary, and many fall inside the 20 km buffer zone. The name of the layer inside the geodatabase is "Fire_Ignitions". It is projected at the Projected Coordinate System: Greek_Grid

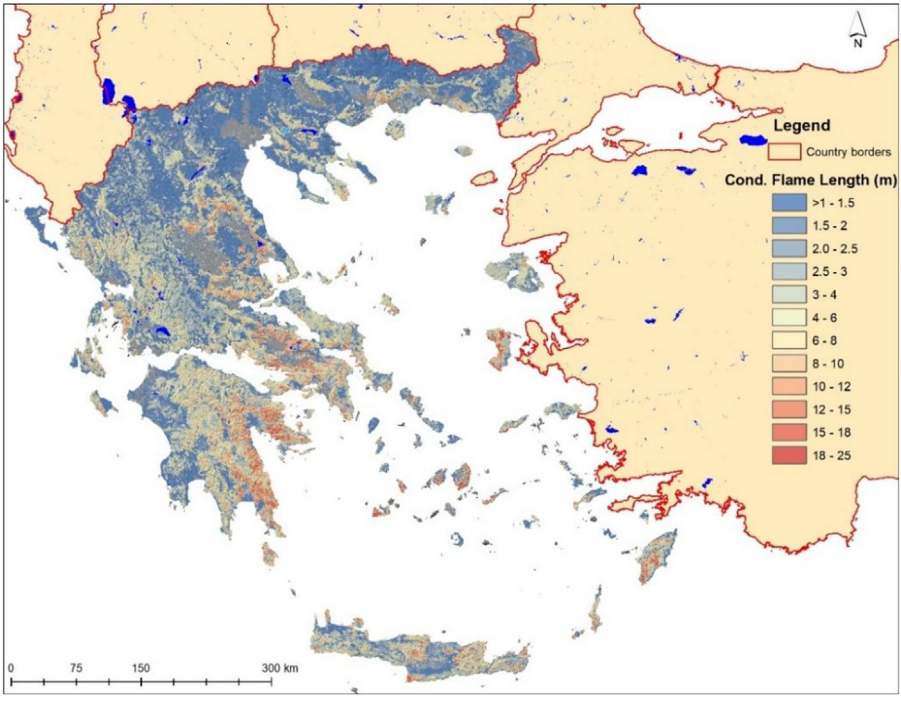

Fig. 4. Conditional Flame Length (m) raster dataset.

(GCS_GGRS_1987); Projection: Transverse_Mercator; Datum: D_GGRS_1987. The attribute table is the same with the simulated fire perimeters, with the only difference being the field "raw_n_HU". This field contains information about the number of buildings exposed to simulated fires, estimated by intersecting the fire perimeter layer with the Microsoft building footprints layer derived from Maxar and Vexcel imagery between 2017 and 2024 [5], and counting the number of the intersections which are recorded in a new data table field. Results were used to create the Structure Exposure Index raster layer.

3.6. Conditional flame length

This is a raster layer of the entire Greek territory at 100 m spatial resolution (Fig. 4), with 7555 Columns and 7597 Rows, depicting the conditional flame length in meters. The name of the layer inside the geodatabase is "CFL". It is projected at the Projected Coordinate System: Greek_Grid (GCS_GGRS_1987); Projection: Transverse_Mercator; Datum: D_GGRS_1987. The pixel type is 32 Bit floating point. Null cell values indicate that on that cell, no fires were simulated due to the non-burnable fuel model assigned to it. The accompanying Layer file (.lyr) contains the proposed colors for 12 classes (1: >1 – 1.5; 2: >1.5 – 2; 3: >2 – 2.5; 4: >2.5 – 3; 5: >3 – 4; 6: >4 – 6; 7: >6 – 8; 8: >8 – 10; 9: >10 – 12; 10: >12 – 15; 11: >15 – 18; 12: >18 – 25).

3.7. Burn probability

This is a raster layer of the entire Greek territory at 100 m spatial resolution (Fig. 5), with 7555 Columns and 7597 Rows, depicting the annual burn probability. The name of the layer inside the geodatabase is "Burn_Prob". It is projected at the Projected Coordinate System:

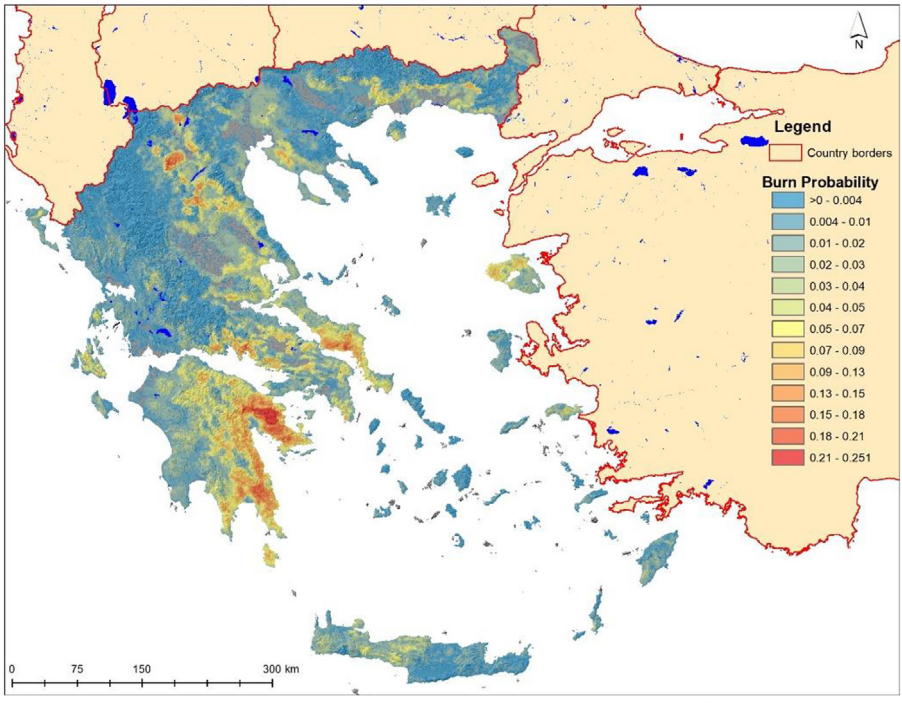

Fig. 5. Annual Burn Probability raster dataset.

Greek_Grid (GCS_GGRS_1987); Projection: Transverse_Mercator; Datum: D_GGRS_1987. The pixel type is 32 Bit floating point. Null cell values indicate that on that cell, no fires were simulated due to the non-burnable fuel model assigned to it. The accompanying Layer file (.lyr) contains the proposed colors for 13 classes (1: >0 – 0.004; 2: >0.004 – 0.01; 3: >0.01 – 0.02; 4: >0.02 – 0.03; 5: >0.03 – 0.04; 6: >0.04 – 0.05; 7: >0.05 – 0.07; 8: >0.07 – 0.09; 9: >0.09 – 0.13; 10: >0.13 – 0.15; 11: >0.15 – 0.18; 12: >0.18 – 0.21; 13: >0.21 – 0.251).

3.8. Structure exposure index

This is a raster layer of the entire Greek territory at 100 m spatial resolution (Fig. 6), with 7541 Columns and 7592 Rows, depicting the total number of structures (not annualized) expected to be exposed by a potential ignition on each pixel by all simulated fires. The name of the layer inside the geodatabase is “Struct_Exp_Index”. It is projected at the Projected Coordinate System: Greek_Grid (GCS_GGRS_1987); Projection: Transverse_Mercator; Datum: D_GGRS_1987. The pixel type is 32 Bit floating point. Null cell values indicate that on that cell, no fires were simulated due to the non-burnable fuel model assigned to it. The accompanying Layer file (.lyr) contains the proposed colors for 13 classes (1: >0 – 100; 2: >100 – 200; 3: >200 – 300; 4: >300 – 400; 5: >400 – 600; 6: >600 – 800; 7: >800 – 1000; 8: >1000 – 1250; 9: >1250 – 1500; 10: >1500 – 2000; 11: >2000 – 2500; 12: >2500 – 5000; 13: >5000 – 10,500).

3.9. Fire size potential index

This is a raster layer of the entire Greek territory at 100 m spatial resolution (Fig. 7), with 7543 Columns and 7592 Rows, depicting the average fire size in hectares of ignitions simu-

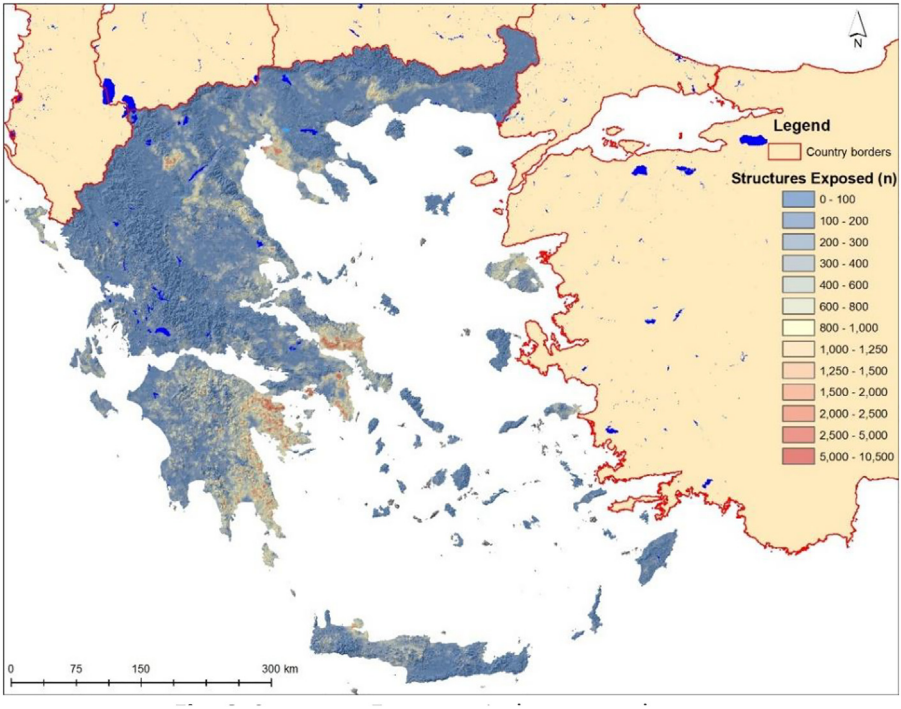

Fig. 6. Structure Exposure Index raster dataset.

lated to start in each cell. The name of the layer inside the geodatabase is "FSP_Index". It is projected at the Projected Coordinate System: Greek_Grid (GCS_GGRS_1987); Projection: Transverse_Mercator; Datum: D_GGRS_1987. The pixel type is 32 Bit floating point. The accompanying Layer file (.lyr) contains the proposed colors for 13 classes (1: >1 – 100; 2: >100– 250; 3: >250 – 500; 4: >500 – 800; 5: >800 – 1250; 6: >1250 – 1750; 7: >1750 – 2250; 8: >2250 – 2750; 9: >2750 – 4000; 10: >4000 – 6000; 11: >6000 – 7500; 12: >7500 – 10,000; 13: >10,000 – 38,200).

4. Experimental Design, Materials and Methods

4.1. Study area

Greece's forested landscape exemplifies the characteristics of a Mediterranean climate, shaped by the mountainous terrain with nutrient-poor soils, and prolonged dry seasons. Human activity, which has influenced the region for over three thousand years, is evident in the current distribution of plant species and the degraded state of many forests. Currently, approximately 21 % of Greece, about 2.8 million hectares, is classified as forested land. Nonetheless, less than half of this area consists of tall, timber-producing forests, predominantly coastal conifer forests at lower elevations. The rest comprises low-growing or coppice forests, mainly used for fuelwood production. Additionally, around 3.2 million hectares are semi-forested zones and shrublands, largely occupied by evergreen broad-leaved shrubs and trees. The landscape also includes roughly 1.9 million hectares of phrygana and grasslands. Phrygana is an east Mediterranean variant of garrigue/scrub, characterized by short and thorny shrubs such as *Phlomis fruticosa, Eu-*

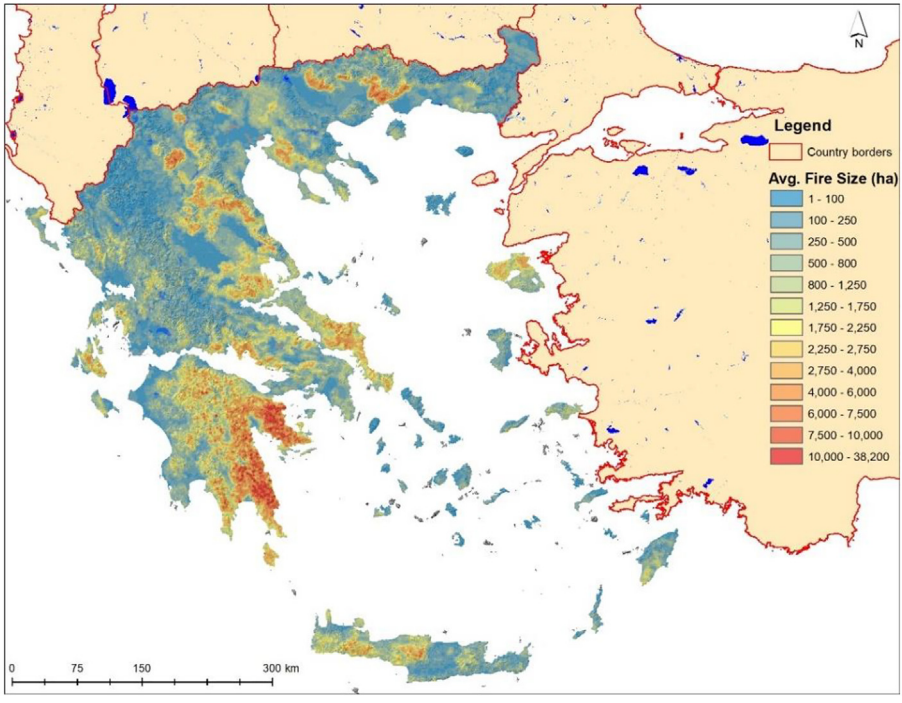

Fig. 7. Fire Size Potential Index raster dataset.

phorbia acanthothamnos, Sarcopoterium spinosum and various Cistaceae and Labiatae, including ericoids and thyme species, mostly utilized for grazing and apiculture.

The lower altitudes of Greece are dominated by drought-resistant evergreen broad-leaved species including *Laurus nobilis, Quercus coccifera, Ceratonia siliqua, Quercus ilex, Arbutus* spp., *Olea europaea* and *Pistacia* spp., alongside pine trees like *Pinus halepensis, Pinus pinea* and *Pinus brutia* in the alliance Oleo-Ceratonietum of the vegetation subzone Quercion ilicis. This alliance extends up to 300 m in the northern regions and up to 800 m in the south. The expanding area of Oleo-Ceratonietum represents the driest regions of Greece. It appears in the lowlands of Crete, the islands of the southern Aegean, southeastern Peloponnese, and Attica. In these areas, the natural vegetation has been degraded for a very long time. Where there are no crops (usually olive groves), phrygana or maquis are present. This vegetation is characterized by herbaceous and low woody species, which typically have no leaves in summer or possess leathery leaves with high concentrations of essential oils. The Oleo-lentiscetum alliance occurs in southeastern and eastern Peloponnese, Attica, eastern Greece up to Pelion, and the Chalkidiki Peninsula. In this area, *Pinus halepensis* forms robust forests. In addition to olive, citrus, and pistachio crops, the growing area features shrubbery with *Olea europaea* subsp. *sylvestris, Pistacia lentiscus, Erica manipuliflora, Quercus coccifera, Lonicera etrusca*, and in more humid areas, *Myrtus communis* and *Nerium oleander. Pinus halepensis* and *P. brutia* thrive in this alliance.

The Andrachno-Quercetum ilicis alliance occupies the lowest areas in western Greece and in eastern Greece up to Mount Orthi, it appears above the Oleo-lentiscetum zone, where *Arbutus unedo, Erica manipuliflora, Quercus ilex* are the dominance species. The Orno-Quercetum ilicis zone occupies the highest area of Quercion ilicis in western Greece, while in eastern Greece, it appears on the eastern foothills of Pelion, Ossa, and Olympus above the Oleo-lentiscetum and on the coasts of Macedonia and Thrace. *Quercus ilex, Fraxinus orneus, Phillyrea latifolia,* and *Quercus coccifera* dominate in this alliance, while olive cultivation is at its coldest.

Moving upward, the next vegetation zone features deciduous broad-leaved species such as *Quercus* spp., *Castanea sativa, Tilia tomentosa*, as well as conifers like *Pinus nigra*, and *Cupressus sempervirens* (in Crete island), which reach up to 900 m in the north and approximately 1200 m in the south parts of Greece. At higher elevations, up to 1800 m, the vegetation comprises of cold-tolerant broadleaves including *Fagus sylvatica*, along with species like *Populus tremula, Betula pendula*, and various *Acer* species, as well as conifers such as *Pinus sylvestris* and *Abies cephalonica*. The highest zones, up to 2200 m, are characterized mainly by conifers tolerant to the cold conditions found there, like *Picea abies, Pinus heldreichii, Pinus sylvestris* and *Pinus peuce*, with a few broadleaf species such as *Sorbus aucuparia*.

Over the past thirty years, Greek landscapes have undergone profound transformations due to extreme wildfire events (EWE) or mega-fires that have resulted in unprecedented environmental and social impacts. The series of major fire seasons, most notably in 2007, 2021, and 2023, have challenged the conventional approaches of management, revealing how these extreme events have reshaped both the physical environment and societal responses. Historically, Greece's annual burned area averaged around 40,000 hectares from about 1500 fires over the last four decades. However, certain years have stood out due to their catastrophic scale: the late 1980s saw fires in 1985 with roughly 105,450 hectares burned, and in 1988 with approximately 110,501 hectares. The year 2000 recorded over 145,000 hectares, while 2007 experienced an extraordinary burn area of 225,734 hectares. That year was marked by significant wildfires in regions such as Achaea (30,000 ha), Laconia (22,000 ha), Messenia (11,000 ha), and Ilia, which experienced multiple fires totalling over 110,000 hectares. Evia also suffered a notable event with 18,000 hectares affected. Attica faced its worst wildfire in 2009, with 20,500 hectares burned, impacting densely populated suburban areas. The year 2021 marked Greece's first mega-fire, devastating over 45,000 hectares in northern Evia, with the overall burned area in the entire country reaching 108,418 hectares according to data from the European Forest Fire Information System (EFFIS). The destruction of extensive forested lands, especially on isolated islands, has far-reaching consequences, including increased risks of flooding, soil erosion, rockfalls, and land degradation, which may take decades to recover.

In 2022, the Hellenic Fire Service responded to a total of 9856 fire incidents, encompassing both agricultural and wildfire events. On average, this translated into roughly 27 fires daily, resulting in approximately 28,500 hectares of land burned. The following year, 2023, saw a slight decrease in the number of ignitions, with 8257 recorded incidents, about 23 fires per day, and a total burned area of around 177,000 hectares. Remarkably, only two ignition events in 2023 accounted for roughly 60 % of the year's total burned area, highlighting the disproportionate impact of a few large fires. July 2023 was particularly notable for a series of intense wildfires across Greece, especially between the 15th and 31st Seven major wildfires ravaged regions including Corfu, Aigio, Dervenochoria, Attica/Kuvaras, Karystos, Nea Anchialos, and Rhodes, collectively burning nearly 47,000 hectares. While the total number of ignitions in 2022 was higher by approximately 1600 incidents, the total area affected in 2023 was nearly four times larger, emphasizing a disturbing paradox: an increase in burned area despite fewer incidents. This discrepancy underscores a significant challenge for wildfire management and highlights the increasing severity of these events. Another notable extreme wildfire event occurred in 2023 when a fire in Evros, northern Greece, burned over 93,500 hectares. This was the largest recorded in Europe over the past two decades and persisted for two weeks, generating smoke that drifted up to 2000 km away from the fire front. In 2024, the total burned area was recorded at 48,307 hectares from 9777 fire incidents, of which 25,550 hectares were forested or covered with vegetation. On the outskirts of Athens, the Varnavas wildfire consumed 8500 hectares of shrublands, cultivated lands, conifer forests, and regrowth areas, largely covered by *Pinus halepensis* saplings, eventually encroaching into urban zones. Meanwhile, the fire at Rozena in Corinth affected 5800 hectares, primarily conifers (around 2000 hectares) and agricultural croplands, which extended over roughly 20,000 hectares.

As Greece faces an increasing likelihood of mega-fires, it is anticipated that similar major wildfires will strike not only regions traditionally susceptible to large-scale fires, such as the Peloponnese, Attica, and Evia, but also higher elevation ecosystems in Central Greece and Epirus.

These ecosystems are particularly vulnerable due to their limited resilience, a consequence of both the presence of fire-sensitive vegetation and the ongoing depopulation, land abandonment, and subsequent fuel accumulation. This situation results in fewer natural fire breaks and higher risks of devastating fires. Essentially, no part of Greece can confidently claim to be immune to mega-fires. A wildfire lasting merely 2–3 hours can lead to tragic loss of life, as seen in the Mati fire in Attica. Large scale events can devastate vast areas of forest, such as the 93,500 hectares burned in Evros, initiating chain reactions of environmental destruction and increasing vulnerability to disasters like flooding, soil erosion, and landslides.

4.2. Stochastic fire simulations

For Greece, we used the FSim fire spread simulator [6] to ask where potential future fires can ignite and how they are expected to propagate. Quantitative wildfire risk analysis requires complete geospatial coverage of fire impact probability and sizes. Wildfire simulation is the primary means of estimating these, including the frequency distribution of large fire events. These simulations can in turn be used to estimate community exposure and ecosystem risk and their results can aid in the planning for potential preventive measures to reduce the estimated fire spread rate and intensity.

FSim simulates the growth and behavior of hundreds of thousands of fire events for risk analysis across large land areas using geospatial data on historical fire occurrence, weather, terrain, and fuel conditions. The effects of large fire suppression on fire duration and size are also simulated. The FSim simulation process involves the following: 1. Assembly of geospatial landscape and terrain data; 2. Assembly and processing of historical fire occurrence data (Fire Occurrence Database); 3. Assembly and processing of historical weather observations (WIMS, FireFamily Plus). Using these datasets, the weather data are analyzed to produce a large number of synthetic 'years' comprising daily weather sequences. For each day of each year the ignitions are stochastically generated, and the growth and behavior of resulting wildfires are simulated as they burn across the landscape. The process continues for the specified number of years, which produces a probability distribution of intensities. These can be summed to obtain the annualized burn probability. Finally, the model results were calibrated by comparison with observed fire distributions.

All FSim simulations were performed at a cell size of 100 m after dividing Greece into 23 macro-areas (Pyromes) that capture changing fire activity gradients based on historical fire activity and climatic stratification of the environment as described by Metzger, et al. [7] (Fig. 1). The number of simulation fire seasons were different at each Pyrome, ranging from 3000 to 71,500 and averaged at 10,000, so that at least 100,000 fires are simulated at each. The Pyromes located at the Greek mainland and Crete received with one set of simulations the requested 100,000, while for Pyromes comprised of islands we followed a slightly different approach. For most major populated islands, we also asked for 100,000 simulations to ensure an adequate number of fires. As a result, islandic Pyromes have more fires since they are comprised of several islands that their simulations are summed. As a sidenote, very small islands, mostly covered with cured herbaceous vegetations and small shrubs, and uninhabited islands and islets did not receive any simulations since the fire danger there is extremely low from human ignitions.

Having more fires for each Pyrome has only two disadvantages, one is that it takes more computational time to perform the simulations, and the second is that burn probability estimates may be more difficult to compare among Pyromes because probabilities are estimated more imprecisely with fewer fires. Lesvos Island with 1600 km^2, for example, had the same number of simulated fires with much larger areas (e.g., Western Greece with 12,000 km^2). Combined with a typical larger fire size in Lesvos compared to Western Greece, they exhibited higher burn probability values. This is an issue discussed and resolved, see the subchapter describing the burn probability estimates. In total, the dataset for the entire Greece contains 3654,905 simulated fires.

4.3. Mapping fuel models and canopy characteristics

Most wildfire behavior models consider numerous empirical variables. While these inputs are important for equation outputs, they are often difficult and time-consuming, if not impossible, to measure for each fuel bed. A fuel model defines these input variables for a stylized set of quantitative vegetation characteristics that can be visually identified in the field. Depending on local conditions, one of several fuel models may be appropriate. In this work we assigned the Scott and Burgan [4] fuel models to the different fuel types of Greece.

As the base mapping layer, we used the CORINE Land Cover (CLC) inventory (2018 version) after intersecting the main forest related classes, i.e., Broad-leaved forest, Coniferous forest, Transitional woodland-shrub and Mixed forest with a detailed vegetation species layer produced by the First National Forest Inventory of Greece that captured the species distribution and cover for reference year 1992 (see Palaiologou, et al. [2] for more details). Then, based on knowledge retrieved through extensive inventories across different Greek ecoregions and expert knowledge regarding the potential fire behavior of each vegetation class, we assigned one or more fuel models at each class depending on topographic and other conditions.

For example, olive groves received three different fuel models depending on the slope of each pixel considering that smaller slopes are easier to treat and maintain in a low fuel state by their owners ($\leq 5°$; Fuel Model: GR1, Short, sparse dry climate grass), compared to those pixels with slopes between 5–15° (FM: GS1, Low load, dry climate grass-shrub) and $>15°$ (FM: GS2, Moderate load, dry climate grass-shrub), where fuel is usually comprised of tall grass mixed with short shrubs and other vegetation.

Similarly, grasslands burn differently across the elevation gradient, with higher altitudes being moister and with different plant properties, i.e., density, height, mixture with shrubs, dead fuel moisture of extinction and curing period. We assigned five different fuel models to grasslands and pastures based on the elevation gradient where the pixel was located, i.e., 0–600 m: GS2, >600–800 m: GS1, >800–1200 m: GR4, >1200–1700 m: GR2, and >1700 m: GR1 (see Table 1 for fuel model definitions). All pixels from the European Settlement Map Built-up areas, after resampling, were assigned with a non-burnable fuel model since those areas are mostly residential buildings or roads. To account for incoming and outgoing simulations ignitions from other countries, and to avoid edge effects during the simulations i.e., having all simulations technically stopping at the country borders, we extended the mapping landscape by 20 km at the northern borders of the country, entering Albania, North Macedonia and Bulgaria since we have evidence of past actual fires that crossed the borders with these countries. For the case of Turkey, this was not necessary since the land border is separated by the river Evros and the borderline on the banks of the river is covered by cultivations, so, the probability of fire spread between the two countries is extremely low. The final fuel model map is presented in Fig. 2.

The most widespread fuel model for forested areas is the TL6, assigned mostly to mixed broad-leaved forests (5.4 % of the total Greek territory), *Quercus* spp. (4.24 %) and *Fagus* spp. (1.5 %) (Table 1). Next, TU1 was assigned to transitional woodland-shrub dominated by *Quercus* spp. (3.9 %), sparse vegetation dominated by *Quercus* spp. (1.3 %) and agricultural lands mixed with sparce *Quercus* spp. and other natural vegetation (1.4 %) and broadleaf shrubs (0.5 %). The TU5 was primarily assigned to *Pinus* spp. (2.5 %), mixed broadleaf-coniferous forest (1.2 %), *Pinus halepensis* (1.5 %) and transitional woodland-shrub dominated by *Abies* spp. (0.7 %). The TL9 was assigned mostly to high elevation conifers, such as *Abies* spp. (1.7 %), and mixed broadleaf-*Abies* spp. (0.4 %). Last, the TU4 fuel model was assigned mostly to sparse *Pinus halepensis* (1.10 %). Regarding the non-forest fuel models, GS1 was assigned to natural grasslands with sparse wooden vegetation (8.2 %), land principally occupied by agriculture, with significant areas of natural vegetation (5.4 %), complex cultivation patterns (5.2 %) and olive groves (5 %). The SH5 was assigned to sclerophyllous vegetation (11.9 %), natural grasslands with significant area covered with shrub (1.3 %) and mixed forest with shrub understory (1 %). The GR1 was assigned to non-irrigated arable land (8.9 %), pastures (0.85 %) and vineyards (0.6 %). The GS2 was assigned to discontinuous urban fabric (1.6 %), agricultural areas with natural vegetation and significant area covered

Table 1
Fuel models distribution over the Greek landscape.

Fuel Model Type	Description	Area (km^2)	Percent
GS1	Shrubs are about 1-foot high, low grass load. Spread rate moderate; flame length low.	36,490	24.68
SH5	Heavy shrub load, depth 4 to 6 feet. Spread rate very high; Flame length very high.	21,104	14.28
TL6	Moderate load, less compact. Spread rate moderate; Flame length low.	16,833	11.39
GR1	Grass is short, patchy, and possibly heavily grazed. Spread rate moderate; flame length low.	15,966	10.80
TU1	Fuel bed is low load of grass and/or shrub with litter. Spread rate low; flame length low.	10,760	7.28
TU5	Fuel bed is high load conifer litter with shrub understory. Spread rate moderate; flame length moderate.	9501	6.43
NB3	Agricultural field, maintained in non-burnable condition.	9323	6.31
GS2	Shrubs are 1 to 3 feet high, moderate grass load. Spread rate high; flame length moderate.	5830	3.94
SH7	Very heavy shrub load, depth of 4 to 6 feet. Spread rate lower than SH5, but flame length similar. Spread rate high; flame length very high.	4372	2.96
TL9	Very high load broadleaf litter; heavy needle-drape in otherwise, sparse shrub layer. Spread rate moderate; flame length moderate.	3098	2.10
GR4	Moderately coarse continuous grass, average depth about 2 feet. Spread rate very high; flame length high.	2994	2.03
NB8	Open water	2530	1.71
TU4	Fuel bed is short conifer trees with grass or moss understory. Spread rate moderate; flame length moderate.	1941	1.31
SH1	Low shrub fuel load, fuel bed depth about 1 foot; some grass may be present. Spread rate very low; flame length very low.	1800	1.22

with shrub (1.3 %) and sparse vegetation with shrubs (0.55 %). The GR4 was mainly assigned to natural grasslands (1.6 %). Finally, the SH1 was assigned to fruit trees and berry plantations (1 %) and pastures with sparse and short shrubs (0.15 %).

For stand height, we used the ETH Global Canopy Height 2020 [8], which is a product that fused the GEDI with Sentinel-2 though probabilistic deep learning model to retrieve stand height at 10 m ground sampling distance for the year 2020. Tree canopy cover was retrieved from the Copernicus portal, showing the level of tree cover ranging from 0 (all non-tree covered areas) to 100 % for the reference year 2018 in 10 m spatial resolution. For Canopy Bulk Density we used the work of Kutchartt, et al. [1] that was conducted within the EU funded project "FIRE-RES". Kutchartt, et al. [1] used the above-ground biomass (AGB) to extract the canopy bulk density (CBD), which is the amount of thin biomass in the trees - i.e., highly flammable fuel. Bulk density refers to the amount of thin biomass per unit volume of the canopy. Thin biomass is mostly leafing biomass (mostly leaves and small twigs), thus AGB without trunk and branch biomass. To estimate thin biomass, allometric models were used to infer the fraction of foliage biomass from the total AGB. Species specific models were used to estimate the foliage biomass according to the compendium equations provided by Forrester, et al. [9]. The value of the fraction is species-specific and depends on the size and age of the tree, but also on the forest management plans in the case of forest plantations. To account for the former, they used a map of tree species probability [10], while tree size and age were estimated by using the canopy height map by Lang, et al. [8] and inverse allometric models to derive diameter. Therefore, a set of biomass equations at tree components provided the fraction of thin biomass (foliage) for different tree species based on diameters as an explanatory-variable [9].

Canopy base height (CBH) was also derived from the work of Kutchartt, et al. [1]. Once the biomass of the thin fuel components was determined, it was possible to determine the density

using canopy volume as the denominator. Canopy volume was determined using tree height and the estimated CBH. Subtracting CBH from total tree height provided the canopy volume. Therefore, canopy fuels are fundamental variables considering that fire usually starts from the ground and increases in intensity and spread rate if it can reach the crown easily, especially when it is near the ground (understory fuels). Therefore, the procedure included three main raster maps, such as tree species, canopy height and aboveground biomass that were combined with different species specific allometric equations including only 16 tree species for predicting the branch insertion height and foliage biomass.

Lastly, using the University of Maryland Forest Loss per Year [11], we retrieved the locations of pixels that faced forest loss during the fire years of 2019 and 2020 and assigned the fuel model GS1 to describe the conditions that prevail after a disturbance, mostly wildfires in our case, that is characterized by a mixture of tall, cured grasses during the summer mixed with short shrubs (including all fires that burned till the end of the 2020 fire season). For disturbances occurred after the reference year of 2018 for canopy cover, we assigned a pixel value of zero. All raster datasets, both the inputs and the final layers, were resampled at 100 m spatial resolution.

4.4. Meteorological data of the study area

Hourly data of 2 m air temperature, 2 m dewpoint temperature, incident solar radiation, precipitation, and 10-m northward and eastward wind components were obtained for the years 2000–2021 from the state-of-the-art global reanalysis dataset ERA5-Land (Muñoz-Sabater 2019) available in the C3S Climate Data Store (CDS). This dataset has a horizontal resolution of 0.1° x 0.1° (about 9 km), an hourly temporal resolution and covers the period from 1950 to present. Relative humidity needed as input to the software FireFamily Plus [12] was computed from air and dew-point temperatures, while wind speed and direction was calculated from its components. It is a known fact that wind speed is underestimated by reanalysis datasets since it averages them out because of its coarse resolution. We used the outcome wind speed with that consideration since it was the only available state-of-the art dataset that had all the required variables for FireFamily Plus, with hourly timestep and higher spatial resolution compared to other available datasets.

A Principal Component Analysis (PCA) was performed on air temperature at 2 m above the surface of land to identify representative data points (used as proxy to weather stations since we did not have real stations with the required data range in our disposal), defined as those with the highest PCA loading, on each Pyrome (23 in total). PCA was performed for the months from May to September and for the period 2000–2020. Moreover, to achieve a sufficient geographic distribution of the fire danger over Greece, more than one data points were considered for some Pyromes, specifically for the North Aegean and the Ionian Islands (see Table 2). Fig. 8 illustrates the representative data points on each Pyrome as identified by PCA as well as the additional data points. Red entries indicate the final selected data points over the Pyromes, and black entries denote the corresponding elevation according to the GMTED2010 digital elevation model (USGS EROS Archive – GMTED2010), upscaled at 9 km spatial resolution.

4.5. FireFamily plus and post-process of meteorological data

FireFamily Plus (FFP) is a software package specifically developed to analyze fire weather data and compute a set of fire danger indices according to the United States National Fire Danger Rating System (NFDRS) [12]. This software incorporates the certified NFDRS codes of 1978, 1988, 2016, as well as the Canadian Forest Fire Danger Rating System (CFFDRS) and the Fosberg Fire Weather Index (FFWI). Using hourly or daily fire weather observations, FFP provides all model calculations to produce fuel moistures and fire danger indices and its principal advantage, among others, is that fire danger can be analyzed as a measure that can assist daily fire related routines

Table 2
General information for each data point in units required by FireFamily plus.

Pyromes	Lon. (deg.)	Lat. (deg.)	Elev. (ft)	Asp. (deg.)	Slope (%)	Slope position	Climate Class	Green-up date	Earliest freeze date	Start KBDI	Start Fuel Moisture 1000	Avg. Prec. (in)	FM
Peloponnese East	22.8	36.9	1302	167	4.5	M: mid	3: subhumid-humid	15/2	31/12	100	25	21.9	G
Vardaris	22.5	40.8	538	198	2.25	L: lower	3: subhumid-humid	3/7	31/12	100	25	26.6	G
Aegean Central	25.2	37	348	166	9.53	L: lower	1: arid-semiarid	15/12	31/12	100	15	15.2	G
Western Greece	20.7	39.3	1870	125	13.7	M: mid	3: subhumid-humid	9/4	31/12	100	25	56.6	G
Macedonia West	21.8	40.5	2733	233	4.7	U: upper	3: subhumid-humid	22/4	31/12	100	25	29.3	G
Macedonia East	23.6	41.1	846	177	15.8	L: lower	3: subhumid-humid	12/4	31/12	100	25	30.7	G
Central Greece	23	38.5	315	61	0.14	L: lower	2: subhumid	4/7	31/12	100	20	24.5	G
Thessaly Coastal	22.9	39.5	1171	196	22.2	M: mid	2: subhumid	9/3	31/12	100	20	31.1	G
South Aegean	27.9	36.3	778	82	2.1	L: lower	2: subhumid	28/2	31/12	100	20	23.9	G
Peloponnese West	21.8	37.3	991	179	7.3	L: lower	3: subhumid-humid	2/3	31/12	100	25	36.7	G
Peloponnese Central	22.2	37.7	2828	289	11.5	U: upper	3: subhumid-humid	9/3	31/12	100	25	32.9	G
Pindos North	21	40.2	3488	53	13.9	U: upper	3: subhumid-humid	2/5	31/12	100	25	37.2	G
Pindos South	21.9	38.8	4347	325	16.1	U: upper	3: subhumid-humid	6/5	31/12	100	25	43.6	G
Thessaly Central	22.2	39.6	797	120	7.2	L: lower	2: subhumid	3/7	31/12	100	20	22.7	G
Rodopi	24.3	41.4	3045	166	8.6	U: upper	3: subhumid-humid	28/4	31/12	100	25	37.6	G

(*continued on next page*)

Table 2 (*continued*)

Pyromes	Lon. (deg.)	Lat. (deg.)	Elev. (ft)	Asp. (deg.)	Slope (%)	Slope position	Climate Class	Green-up date	Earliest freeze date	Start KBDI	Start Fuel Moisture 1000	Avg. Prec. (in)	FM
Thraki North	25.7	41.3	1860	340	9.9	M: mid	3: subhumid-humid	22/4	31/12	100	25	32.1	G
Thraki South	26.1	41	692	61	3.3	L: lower	3: subhumid-humid	16 /4	31/12	100	25	31.1	G
Crete West	24.6	35.2	1900	11	26.3	M: mid	1: arid-semiarid	10/3	31/12	100	15	19.4	G
Crete East	25.73	35.08	1378	263.7	46.4	M: mid	1: arid-semiarid	31/1	31/12	100	15	11.2	G
Evia island	23.87	38.55	1247	295.6	37.5	M: mid	1: arid-semiarid	1/4	31/12	100	15	25.5	G
Attica	23.88	38.15	971	63	13.0	L: lower	1: arid-semiarid	22/2	31/12	100	15	19.8	G
Data points for Ionian Islands Pyrome													
Cephalonia island	20.49	38.28	1985	292	39.5	M: mid	3: subhumid-humid	03/3	31/12	100	25	36.1	G
Corfu island	19.83	39.61	89	42	8.9	L: lower	3: subhumid-humid	6/4	31/12	100	25	51.5	G
Data points for North Aegean Pyrome													
Samos island	26.80	37.73	1447	81.8	10.0	M: mid	2: subhumid	14/4	31/12	100	20	37.7	G
Lesvos island	26.28	39.26	794	295	5.7	L: lower	3: subhumid-humid	4/2	31/12	100	25	27.3	G
Chios island	26.1	38.5	620	74	9.1	L: lower	3: subhumid-humid	3/2	31/12	100	25	23.4	G

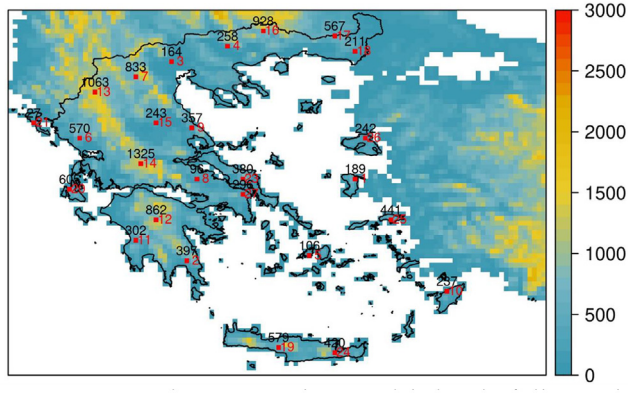

Fig. 8. Representative data points over each Pyrome and islands, as identified by Principal Component Analysis. Red entries indicate the representative data point and black numbers the corresponding elevation (in meters above sea level). Colors indicate the elevation in meters.

and tasks [12,13]. In this analysis, we used the most recent version of FFP (Version 5) and the 1978 version of the NDFRS model, employing hourly meteorological data. A number of dummy stations, equal to the number of assigned data points (Table 2), should be created prior to importing the meteorological data into the FFP. Table 2 provides the general information for each data point, and the assigned values are explained in the subsequent paragraphs.

4.5.1. General data point information

Aspect represents the exposure of the slope on which the data point is located. Aspect values are classified into nine classes with the first one indicating no slope (flat) and the rest eight classes denoting the directions the physical slopes face [13]. It is measured clockwise in degrees from 0 to 360. In FFP, each class is labelled with a one-digit code from 1 to 8 where slope exists and 0 for flat terrain: 0 – flat/none, 1 – northeast (45°), 2 – east (90°), 3 – southeast (135°), 4 – south (180°), 5 – southwest (225°), 6 – west (270°), 7 – northwest (315°), and 8 – north (360°). The aspect for the selected data points was calculated using GIS software based on the GMTED2010 digital elevation model, and then the abovementioned classes were assigned.

The slope describes the increase or reduction of the terrain slope measured in the number of feet change per 100 feet (approximately 30.5 m) of horizontal distance, and it is expressed as percentage. According to the NFDRS, the slope is classified into five classes: 0–25, 26–40, 41–55, 56–75, and greater than 75 % [13,14]. Each class is labelled with a one-digit code from 1 to 5. The slope of the data points was calculated using GIS based on the GMTED2010 digital elevation model, and then it was assigned to one of the five classes.

The slope position describes the general location of the data point, and it is grouped into three classes: lower (valley bottom or flat), mid (mid-slope), and upper (ridge or peak) [13]. This parameter was defined using suitable elevation levels according to the study of Pluntke, et al. [15]. Therefore, data points with elevation lower than 350 m were classified into the lower class, with elevation between 351 and 650 into the mid class, and with elevation greater than 650 into the upper class.

The climate class describes the general climate of the area to define the drying and wetting rates of the underlying vegetation. It is recognized that vegetation adapts to the climatic conditions of an area and that in some extend, it affects the seasonal fire danger [13]. According to the NFDRS, climate is classified into four classes to meet danger-rating needs: 1 – arid/semiarid, 2 – sub-humid, 3 – sub-humid/humid, and 4 – wet [13,14]. In order to assign a climate class to the examined data points, the classification of Nastos, et al. [16] based on the spatial distribution of the Aridity Index was used. Nastos, et al. [16] calculated the Aridity Index (AI) for Greece for the period 1991–2000 based on observational data of temperature and precipitation and de-

fined different climate zones for Greece based on the United Nations Environment Programme AI classification.

The green-up date describes the beginning of a new cycle of plant growth and signals the start of the green-up processes. To assign the green-up date for each data point, the High-Resolution Vegetation Phenology and Productivity (HR-VPP) product suite of the Copernicus Land Monitoring Service (CLMS) was utilized. The HR-VPP comprise of 13 parameters characterize the vegetation growth cycle and are available at a horizontal resolution of 10 m resolution for the period from 2017 until today, with yearly updates. In our analysis, the day of the "start of the growing season" (SOSD) parameter was used as a proxy to the green-up date. For each of the examined data points, a growing season start date was determined based on the pixel values of the SOSD parameter (reference year 2022) in a buffer zone of 5 km around each of the examined data points. The earliest freeze date describes the day of the year when the first frost may occur, and it was set constant to the default date (31 December) throughout the selected data points.

The start KBDI parameter represents the initiation value for the Keetch-Byram Drought Index (KBDI). This index is used to describe the effects of seasonal drought on fire potential. When the 1978 version of NFDRS is used, as in our case, KBDI is a stand-alone index whose values are not entered into calculations. However, its initial value is displayed in FFP, and it is a required field. Therefore, a default initiation value of 100 was assigned [13,14].

The start FM1000 parameter represents the startup values for the 1000-hr fuel moisture content. The latter describes the moisture content in the dead fuels consisting of roundwood, three to eight inches in diameter, or the layer of the forest floor more than about four inches below the surface, or both [13,14]. According to the NFDRS, the initiation values of 1000-hr are established based on the climate class as follows: 15 for arid/semiarid class, 20 for sub-humid class, 25 for sub-humid/humid, and 30 for wet class [13,14].

The average precipitation describes the historic average annual precipitation of the data point. It was calculated based on the hourly precipitation data for the period 2000–2021 for the selected data points.

A fuel model intends to represent the quantity and distribution of dead and live plant material. A set of 20 fuel models has been developed for operational use in 1978 NFDRS. These models are referred to using characters from A to U for communication purposes [13,14]. FSim has been explicitly implemented using the fuel model G, since it seems to relate well to the occurrence of large fires, whatever the actual fuel conditions in an area may be [6,17]. Therefore, all estimations in the FFP for the selected data points were performed with the NFDRS fuel model G. This model represents an area with dense conifer stands with heavy accumulation of litter and down woody material, and varying surface short vegetation (see [14,18,19] for more information on the technical details and description of fuel model G).

4.5.2. Import reanalysis data

To import the hourly ERA5-Land reanalysis data into the FFP, we had to generate files in the standard FW9 format. FW9 file is a fixed field text file that comprises a set of weather elements. The elements used and the order in which they appear in this file format are summarized in Table 3.

In this file format, all records begin with the identifier code W98. The data point (i.e., station) number is a unique 6-digit number assigned for identification purposes. The observation type element was set at R type, since we are using hourly data. Maximum and minimum dry bulb temperature and relative humidity indicate the highest and lowest values of each parameter during the preceding 24-hour period. These elements are employed for the adjustment of the standard drying function of the NFDRS algorithms to better reflect actual conditions [14]. The precipitation amount indicates the total amount of precipitation within the preceding 24-hour period. The precipitation duration describes the actual number of hours that precipitation fell in the 24-hour period immediately preceding the observation time. This element is of great importance, since it represents the total time that the fuels are exposed to water [14]. The element of solar radiation is used to describe the amount of sunlight received by fuels in the

Table 3
The order in which the required elements were entered to generate the FW9 file.

Item	Description	Units	Item	Description	Units
1	Record type identifier code (W98)	–	10	Maximum dry bulb temperature	°F
2	Station number	–	11	Minimum dry bulb temperature	°F
3	Observation date	–	12	Maximum relative humidity	%
4	Observation time	–	13	Minimum relative humidity	%
5	Observation type (R, Raws)	–	14	Precipitation duration	hours
6	Dry bulb temperature	°F	15	Precipitation amount	inches
7	Relative humidity	%	16	Moisture type code	–
8	Wind direction azimuth	degrees	17	Measurement type code	–
9	Average wind speed	miles/hour	18	Solar radiation	W/m^2

area of interest, and it is expressed in watts per square meter. The moisture type code indicates the expression of atmospheric moisture used, which in this case is the relative humidity. The measurement type code signifies the system of units used, which in this case is the U.S. system where temperature is expressed in Fahrenheit, wind speed in miles per hour, and precipitation in decimal inches. The generated weather files were populated with the ERA5-Land dataset, covering the period 2000–2021 at an hourly time step.

4.5.3. Output files

FFP incorporates a number of seasonal reports that summarize the seasonal variations of fuel moistures, NFDRS indices, and components [12]. The FlamMap Fire Risk Export option was opted, and the corresponding output files were generated for the selected data points. This type of report provides the Energy Release Component (ERC), the fuel moisture content for dead fuels (1-hr, 10-hr, 100-hr, 1000-hr) and live fuels (herbaceous, woody, 1000-hr fuel moisture value), as well as the wind speed versus wind direction. When generating this type of report, the wind records can be further specified in relation to the years of data, the time of year and the time of day. Therefore, the wind records were set to cover the period 2000–2021 including all months, while the time of day was set between 09:00 and 19:00. The ERC, as a calculated output of this type of report, is an indicator of how much potential energy (Btu) is available to be released per unit area (square foot) in the flaming front [14]. Since it considers both dead and live fuel moistures, it reflects well the drought conditions. Wind is not part of ERC calculation and thus, its daily variation is relatively small. The ERC is a cumulative type of index, and its daily calculation considers the conditions of the past seven days. Its scale is open-ended [14].

4.6. Estimating fire ignitions distribution and human-caused ignition probability

The simulation of realistic fire ignitions based on fire history and the corresponding microclimatic conditions constitute one of the most significant procedures in wildfires simulation. The database with previous locations of fire hotspots in conjunction with a time series analysis of weather data can provide reliable outcomes. To this end, we divided the entire country into broader geographical regions. This division is slightly different from the Pyromes, since we had to merge similar Pyromes to ensure an adequate number of historical ignitions. For example, the Peloponnese constituted one geographical region for fire ignition history, but with three original data points. For each geographical region we used one or more data points (see previous subchapter) to retrieve hourly weather data from 2000 to 2021, including the most contributing factors, such as temperature, relative humidity, 24-hr rainfall, wind speed and direction, maximum and minimum temperature, maximum and minimum relative humidity, solar radiation and hourly precipitation for the entire calendar year. These parameters determine the fire regime for each region. Next, we proceeded with fire probability analysis to determine the probability of large fire ignition (i.e. escaped fire) through FireFamily Plus. Similarly to Finney, et al. [6], we estimated the probability of large fire ignition based on the daily Energy Release Component

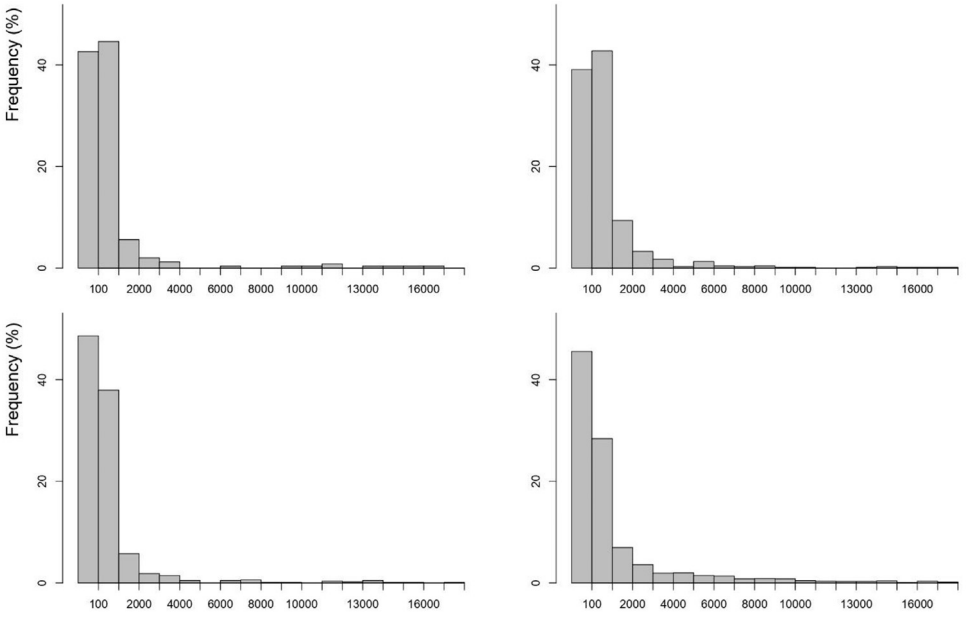

Fig. 9. Comparison between historical (left panels) vs. simulated (right panels) fire size distribution (hectares; x-axis) for Macedonia East (top panels) and Evia (bottom panels) used for model calibration and validation.

(dependent variable). This process occurred by calculating the coefficients of logistic regression that are used to estimate the above probability [17]. The most significant finding here is the estimation of conditional probability for the initiation of at least one large fire, which is differentiated for each region. Empirically, the threshold for a large fire in Greece is 600 ha. The ignition of more than five simultaneous large fires is very rare in Greece.

Human-caused ignition probability was calibrated using Random Forest models based on historical fire location records, retrieved from the Hellenic Fire Service for the years 2017–2022, combined with geospatial layers describing wildland interfaces, land cover types, human pressure (population density) and accessibility (i.e., roads) [20]. The modelling framework relied on presence–absence data, where presence corresponded to observed fire ignitions and absence to locations without recorded ignitions during the study period. Predictor variables were extracted at ignition points to characterize conditions conducive to fire occurrence. Absence points were defined as any location without a recorded fire during the analysis period, and their number greatly exceeded that of ignition points. To address this imbalance, we generated 1000 random absence samples, each containing the same number of observations as the recorded fires. For each sample, an individual RF model was trained and validated. From the ensemble of models, the final candidate was selected as the one with predictive performance closest to the median value of the area under the receiver operating characteristic curve (AUC), representing the average expected performance. The spatial resolution of the dataset was set at 100 m. All raster cells falling inside non-burnable fuel models were assigned with the value of zero, so that no ignitions are allocated there during the simulation process.

4.7. Calibration - validation

The calibration-validation technique compared the size distribution of simulated fires to the historical one of each geographic region (Fig. 9). Even though different measures can be used

to optimize the calibration process, such as the number of large fires per year, the number of large-fire acres burned per year, the mean annual large-fire burn probability, the mean large-fire size, and the agreement with the historical fire-size distribution [17], the last option was chosen since it has successfully tested in previous research projects providing sufficient degree of reliability [21]. A continuous calibration process was carried out before the simulation modelling final products were produced. Several factors may need to be adjusted as part of the calibration process. However, the most significant ones are related to the burning conditions and the fire growth modules, such as calibrating the large-fire size through the adjustment of Rate of Spread (ROS) and the suppression module of FSim.

The suppression module affects the large-fire size, and it constitutes a good tool for calibration. The suppression factor can range from 1 (strong suppression capacity) to 10 (weak suppression capacity). This factor varied based on the geographical region and the respective firefighting capacity. Respectively, ROS was adjusted to the existing fuels in any region. The adjustment involved the configuration of ROS to be higher than 1, which is reflected in the increase of fire rate of spread, whereas ROS lower than 1 indicates reduced surface ROS. Reduced ROS and/or strong suppression will lead to lower mean large-fire size and vice versa [17]. Hence, depending on the specific features of each geographic region, differentiated combinations of the suppression module and the ROS factor were adopted. The selection of optimal values for the above factors made the simulation results present great similarity with the historical fire size distribution. The absolute matching of the two curves should be considered infeasible since the large fire history database for several geographic regions had very few records available. The more coherent and complete the fire history database is, the better the matching of the actual and simulated curves (after the appropriate adjustment).

4.8. Model outputs

FSim generates the fire intensity result as flame length probability (FLP) where pixel-level outputs are expressed for 20 bin 0.5 m fire-intensity levels (FIL1 to FIL20, FIL20 $\geq$ 9.5 m). The probability-weighted fire intensity was estimated with Eq. (1).

$$CFL = \sum_{t=1}^{20} FLP_i \times FL_i \tag{1}$$

where CFL is the conditional flame length (m), FLPi is the flame length probability of a fire at the i th flame length category, and FLi is the flame length (m) midpoint of a 0.5 m flame length 20-bin i th category FIL fire intensity level. The CFL computes all the fire front spreading directions and the respective probability at a given pixel (i.e., heading, flanking, and backing) and proxy of wildfire hazard. It describes the potential for loss given a fire burns a valued resource or asset and allows for assessment of the fire suppression capabilities under the extreme weather conditions assumed to model wildfire behavior. Then, we mosaiced the rasters of the different Pyromes and applied a 3 $\times$ 3 rectangle with focal statistics to estimate the average pixel value.

FSim computes conditional burn probability from the number of simulated fires defined at each Pyrome. The annual burn probability (aBP) represents the annual likelihood of burning given the current landscape and conditions, is estimated as the ratio between BP of a given pixel and the modelled wildfire seasons and can range from 0 (the pixel never burns) to 1 (the pixel burns every wildfire season). Burn probability was estimated with Eq. (2).

$$BP = \frac{F}{n} \tag{2}$$

where, F is the number of times a pixel burns, and n is the number of simulated fires. As explained in the subchapter explaining the different number of fire seasons, islands received more fires than the mainland Pyromes and this caused inconsistencies at the burn probability among the Pyromes. We accounted and corrected this with the following process. During the five-year period of 2017–2022, the Hellenic Fire Service recorded approximately 58,000 ignitions across

the country. We created a 1 km^2 grid and counted the number of fires falling at each grid square. After removing those squares with zero fires, we averaged the number of fires, and we found that we have 17 real ignitions per km^2. We used this number to find the right number of simulations needed based on the area of each Pyrome and then used it to correct the burn probability estimates. For example, Western Greece with an area of 12,055 km^2 had 108,443 simulated fires when it should have 204,937, while the Ionian Islands with an area of 2237 km^2 had 417,694 simulated fires when it should have 38,041. Using the number of fires each Pyrome should have based on its area, we corrected the original burn probability rasters, mosaiced them and then applied a 3×3 rectangle with focal statistics to estimate the average pixel value.

The Fire Size Potential Index (FSPI) shows the average fire size (ha) that can be generated by a potential ignition in each pixel [22]. Here, each simulated fire size was attributed to the respected ignition point, and then the points were smoothed to create a continuous raster coverage. The Structure Exposure Index (SEI) measured the absolute number of structures expected to be exposed from a potential ignition in a given pixel [22]. SEI was created by assigning each ignition point with the number of structures affected by the fire generated from that ignition (a polygon) and smoothing the resulting point map. Structure locations were retrieved from the 2024 version of the Microsoft building footprints layer, derived from Maxar and Vexcel imagery between 2017 and 2024 [5] and intersected with fire perimeters to count how many buildings were inside each. The outputs were created from ArcGIS IDW processes based on fields in the fire ignition attribute table. A power of 1, and a fixed search radius of 2000 m are used for the IDW process. The final rasters are smoothed using a Focal Statistics process that takes the average value within a 7-cell circular radius, with a 100-meter cell size.

4.9. Metadata

For the File Geodatabase, and each of the contents, we created a metadata file with basic and supplementary information through the embedded functionality of ArcCatalog version 10.4. Each metadata was exported as an individual .xml file, using the ARCGIS2ISO19139.xml translator. The ISO 19139 specifies an XML implementation of the ISO 19115 standard for geographic information metadata. It provides a common format for describing and exchanging metadata about geospatial datasets, including information on identification, quality, and extent. This standardization is achieved by defining a set of XML schemas, often called “gmd” (geographic metadata XML), that ensure interoperability among different systems and software. The ARCGIS2ISO19139.xml translates content stored in the ArcGIS metadata format to the ISO 19139 XML format. This translator is used by default when metadata is exported using any of the ISO-based metadata styles. Metadata is converted using an XSLT transformation and won’t produce a log file.

To describe the schema of the File Geodatabase, we generated a schema report with ArcGIS Pro 3.5 to produce readable Excel, JSON, PDF, and HTML reports that describe the dataset structure. Documenting the schema allows for both GIS and non-GIS staff to understand the data and how it relates to other data in their data model. For example, the Excel workbook format provides a table of contents (TOC) tab with an overview of the information included in the report. To quickly navigate to other sections of the workbook, end-users can click the hyperlinked text or use the worksheet tabs along the bottom. All metadata can be accessed and viewed from ArcCatalog for both individual files or through the File Geodatabase, and we provide them in the Zenodo repository as individual .xml files, while for the schema report, files can be opened and viewed directly.

Limitations

The dataset was created considering the surface fuel conditions that occurred during the reference year 2018 since we used the Corine Land Cover layer as a base for mapping. Canopy fuel

conditions are referenced for the year 2020 from their source [1], except for Canopy Cover which is referenced for the year 2018. As a result, all wildfires that burned in Greece for the two fire periods between 2019 and 2020 were considered only by changing the surface fuel model to GS1 and zeroing the canopy cover values.

Limitations exist when the 40 Scott and Burgan fuel models are used outside their domain, which is the continental US, and in our case, when used to translate the Corine Land Cover of Greece (enhanced with corrections and additions from the Greek forest inventory) into fuel models. The 40 Scott and Burgan fuel models have inherent limitations even when applied in the US since they are used with Rothermel's surface spread equations, so they inherit Rothermel's assumptions i.e., homogeneous continuous surface fuel bed, quasi-steady flame front, empirically derived relationships, no explicit spotting, limited crown-fire physics, and simplified wind and slope interactions. As a result, this constrains realism for extreme and complex fires. Real fuelbeds of Greece vary by species, structure, season and management history, so the 40 Scott and Burgan fuel models can be potentially a poor match to local conditions, although we assigned them to the best of our knowledge considering collected information from numerous field inventories we conducted across Greece to identify the correct fuel archetype of each region before applying them. The calibration process ensured that the simulated fire size distribution matched the historical for each Pyrome, even though each individual fire could be simulated better if custom fuel models that depict local fuel conditions were available. Greece can have substantially different fuel arrangements, species fuel chemistry (heat content, flammability), and continuity than the 40 Scott and Burgan fuel archetypes. Grazing, altered fire regimes, invasive species or insect outbreaks, fuel treatments and historical land use change local fuelbeds in ways Scott and Burgan fuel archetypes don't capture.

The 40 Scott & Burgan's fuel models are a major step forward for standardized wildfire modelling, but they are archetypes tied to the Rothermel framework and to assumptions that don't hold everywhere. They're excellent for rapid mapping and consistent workflows, but can produce biased or misleading outputs if used without local validation, seasonal and dynamic adjustments, or calibration, especially outside the USA where vegetation, fuel chemistry, phenology and management differ. The use of locally calibrated custom models with quantified uncertainty, possibly supported with remote sensing and LiDAR and validation against observed fires, is the most effective way to improve simulation realism.

Fires that burned during the five fire periods of 2021–2025 were not considered. We also have not considered the potential natural change of the surface fuel models after the year 2018, and the natural changes in canopy conditions after their reference years (2018 for canopy cover and 2020 for the rest). The users of the dataset should be aware of this and remove fires from that ignited in burned areas of the period 2021–2025. We kept in the final dataset all simulated fires for both validation purposes (how well model performed in real fire events) and for an estimation of how future fires can burn in the same areas if the vegetation and fuel conditions recover to their former (prior to burning) state.

Ethics Statement

The authors have read and follow the ethical requirements for publication in Data in Brief and confirming that the current work does not involve human subjects, animal experiments, or any data collected from social media platforms.

Credit Author Statement

Palaiologos Palaiologou: Conceptualization, Methodology, Data curation, Writing –review & editing, Writing –original draft, Resources. **Christos Giannakopoulos:** Visualization, Investigation, Software, Project administration. **Christos Vasilakos:** Software, Validation, Writing -

Review & Editing. **Stavros Sakellariou:** Resources, Formal analysis, Investigation. **Marcos Rodrigues:** Resources, Formal analysis, Investigation. **Anna Karali:** Visualization, Investigation, Software, Writing - Original Draft. **George Katavoutas**: Visualization, Investigation, Software. **Konstantinos V. Varotsos:** Visualization, Investigation, Software. **Olga Roussou**: Writing - Review & Editing, Validation, Resources. **Pere Joan Gelabert:** Resources, Formal analysis, Investigation. **Adrián Jiménez-Ruano:** Resources, Formal analysis, Investigation. **Giannis Lemesios:** Resources, Investigation**. Antoni Trasobares:** Project administration, Funding acquisition, Supervision. **Mark Finney:** Conceptualization, Software, Methodology. **Kostas Kalabokidis:** Conceptualization, Supervision, Writing –review & editing, Writing –original draft, Project administration.

Data Availability

A dataset to support wildland fire and fuel management in Greece created with stochastic wildfire simulations (Original data) (Zenodo).

Acknowledgements

This research was funded by the European Union's Horizon 2020 Research and Innovation Programme through the project entitled "Innovative technologies & socio-ecological-economic solutions for fire resilient territories in Europe – FIRE-RES" under grant agreement N°101037419.

Declaration of Competing Interest

The authors declare that they have no known competing financial interests or personal relationships that could have appeared to influence the work reported in this paper.

Supplementary Materials

Supplementary material associated with this article can be found, in the online version, at doi:10.1016/j.dib.2025.112304.

References

[1] E. Kutchartt, J.R. González-Olabarria, N. Aquilué, J. Garcia-Gonzalo, A. Trasobares, B. Botequim, M. Hauglin, P. Palaiologou, V. Vassilev, A. Cardil, M.Á. Navarrete, C. Orazio, F. Pirotti, Pan-European fuel map server: an open-geodata portal for supporting fire risk assessment, Geomatica (2024) 100036, doi:10.1016/j.geomat.2024.100036.
[2] P. Palaiologou, K. Kalabokidis, M.A. Day, A.A. Ager, S. Galatsidas, L. Papalampros, Modelling fire behavior to assess community exposure in Europe: combining open data and geospatial analysis, Int. J. Geo-Inf. (2022) 198.
[3] P. Palaiologou, K. Kalabokidis, C. Vasilakos, A geographical analysis of wildfire fuel characteristics by cover type in Greece, in: N.R. Dalezios (Ed.), 2nd International Symposium Agroecoinfo, University of Thessaly, Volos, Greece, 2022, pp. 161–167.
[4] J.H. Scott, R.E. Burgan, in: Standard Fire Behavior Fuel models: a Comprehensive Set for Use with Rothermel's surface Fire Spread Model, USDA Forest Service, Rocky Mountain Research Station, Fort Collins, CO, 2005, p. 72.
[5] Microsoft, Worldwide building footprints derived from satellite imagery, 2024.
[6] M.A. Finney, C.W. McHugh, I.C. Grenfell, K.L. Riley, K.C. Short, A simulation of probabilistic wildfire risk components for the continental United States, Stoch Env Res Ris A 25 (2011) 973–1000, doi:10.1007/s00477-011-0462-z.
[7] M.J. Metzger, R.G.H. Bunce, R.H. Jongman, C.A. Mücher, J.W. Watkins, A climatic stratification of the environment of Europe, Glob. Ecol. Biogeogr. 14 (6) (2005) 549–563.
[8] N. Lang, W. Jetz, K. Schindler, J.D. Wegner, A high-resolution canopy height model of the Earth, ArXiv. preprint arXiv:2204.08322 (2022).
[9] D.I. Forrester, I.H.H. Tachauer, P. Annighoefer, I. Barbeito, H. Pretzsch, R. Ruiz-Peinado, H. Stark, G. Vacchiano, T. Zlatanov, T. Chakraborty, Generalized biomass and leaf area allometric equations for European tree species incorporating stand structure, tree age and climate, For Ecol Manag 396 (2017) 160–175.

[10] C. Bonannella, T. Hengl, J. Heisig, L. Parente, M.N. Wright, M. Herold, S. De Bruin, Forest tree species distribution for Europe 2000–2020: mapping potential and realized distributions using spatiotemporal machine learning, Peer J. 10 (2022) e13728.
[11] M.C. Hansen, P.V. Potapov, R. Moore, M. Hancher, S.A. Turubanova, A. Tyukavina, D. Thau, S.V. Stehman, S.J. Goetz, T.R. Loveland, A. Kommareddy, A. Egorov, L. Chini, C.O. Justice, J.R.G. Townshend, High-resolution global maps of 21st-century forest cover change, Science (1979) 342 (6160) (2013) 850–853, doi:10.1126/science.1244693.
[12] L. Bradshaw, E. McCormick, in: FireFamily Plus user's guide, Version 2.0, Gen. Tech. Rep. RMRS-GTR-67-WWW, 67, US Department of Agriculture, Forest Service, Rocky Mountain Research Station, Fort Collins, CO, 2001, p. 124.
[13] NWCG, WIMS user's guide: chapter 6 - working with station information, in: N.W.C. Group (Ed.) Weather Information Management System User Guide, Boise, ID, 2011, p. 39.
[14] P. Schlobohm, J. Brain, Gaining an understanding of the national fire danger rating system, National wildfire coordinating group, PMS 932 (2002).
[15] T. Pluntke, S. Schwarzak, K. Kuhn, K. Lünich, M. Adynkiewicz-Piragas, I. Otop, B. Miszuk, Climate analysis as a basis for a sustainable water management at the lusatian neisse, meteorology hydrology and water management, Res. Operat. Appl. 4 (2016).
[16] P.T. Nastos, N. Politi, J. Kapsomenakis, Spatial and temporal variability of the Aridity Index in Greece, Atmos. Res. 119 (2013) 140–152.
[17] J.H. Scott, K.C. Short, M. Finney, J. Gilbertson-Day, K.C. Vogler, FSim: the Large-Fire Simulator — Guide to Best Practices Version 0.3.1, 2018.
[18] L.S. Bradshaw, J.E. Deeming, R.E. Burgan, J.D. Cohen, in: The 1978 National Fire-Danger Rating System: Technical documentation, USDA Forest Service, Intermountain Forest and Range Experiment Station, Ogden, UT, 1983, p. 44.
[19] J.E. Deeming, R.E. Burgan, J.D. Cohen, The National Fire-Danger Rating System –1978, USDA Forest Service, , Intermountain Forest and Range Experiment Station, Ogden, UT, 1977.
[20] P.J. Gelabert, A. Jiménez-Ruano, C. Ochoa, F. Alcasena, J. Sjöström, C. Marrs, L.M. Ribeiro, P. Palaiologou, C. Bentué Martínez, E. Chuvieco, C. Vega-Garcia, M. Rodrigues, Assessing human-caused wildfire ignition likelihood across Europe, EGUsphere 2025 (2025) 1–27, doi:10.5194/egusphere-2025-143.
[21] S. Sakellariou, A. Sfougaris, O. Christopoulou, S. Tampekis, Integrated wildfire risk assessment of natural and anthropogenic ecosystems based on simulation modeling and remotely sensed data fusion, Int. J. Disaster. Risk. Reduct. 78 (2022) 103129.
[22] A.A. Ager, P. Palaiologou, C.R. Evers, M.A. Day, A.M.G. Barros, Assessing transboundary wildfire exposure in the southwestern United States, Risk. Anal. 38 (10) (2018) 2105–2127, doi:10.1111/risa.12999.